Quench analysis of large superconducting magnets. Part I: model description

L. Bottura and O.C. Zienkiewicz*

The NET Team, c/o Max Planck IPP, Boltzmannst. 2, D-8046 Garching, FRG
*Institute for Numerical Methods in Engineering, University College of Swansea, Swansea SA2 8PP, UK

Received 26 September 1991; revised 13 January 1992

In large superconducting magnets built using force-flow cooled conductors, such as those being designed for next generation fusion machines, the quench propagation is a three-dimensional phenomenon. In this paper we develop a method for the analysis of quenches in 3-D which is extremely versatile and comprehensive. The method is based on the parallel solution of a set of 1-D problems represented by the helium flow, heat conduction and quench propagation along the conductor length. Transverse heat exchange among conductors is then explicitly inserted in the model, thus achieving the desired 3-D capability. In the model developed for the 1-D analysis we have foreseen the possibility of taking into account the thermal gradients in the cable cross-section, and the changes of magnetic field and operating current which are typical of a quench transient.

Keywords: quench, protection, force-flow superconductors

The analysis of quench propagation for force-flow cooled conductors has always been a matter of fundamental importance for the design of the protection scheme of a superconducting magnet[1]. This is even more true for the large magnets which are under design for fusion machines of the next generation[2]. These magnets will be a considerable investment compared to the cost of the whole plant, and will store an amount of energy in the order of several tens of GJ. Therefore there is an increasing interest in the issues of safety and protection of these systems.

The quench propagation in force-flow cooled superconducting magnets has so far been studied only in a one dimensional (1-D) approximation, assuming that the dominating mode of propagation is that in the longitudinal direction of the cable (along the helium flow). This hypothesis is at the basis of most of the quench analysis codes developed in the last 15 years[3-7].

The one dimensional behaviour is only a simplifying assumption, and should be avoided if a more powerful modelling tool is available. In a real superconducting magnet, the initiation and the propagation of a normal zone depend not only on the longitudinal heat fluxes, but also on the heat diffusion in the winding pack cross-section, i.e. transverse to the main conductor axis. A normal zone can be initiated by heat conduction in turns or pancakes adjacent to the one initially quenched, thus increasing the normal zone propagation speed in the coil and decreasing the thermal gradients among neighbouring conductors. Therefore, one can expect that the calculations of the quench propagation and of the hot-spot temperature performed with the 1-D models are generally conservative, as in this approximation the energy deposition tends to be concentrated in the cable region initially quenched. For the cable design this means over-dimensioning the stabilizer and therefore losing efficiency. Furthermore, in the case of uncontrolled transients, the calculation performed in the 1-D approximation may predict catastrophic events that are not realistic, such as the loss of insulation or melting of the cable. The question of the relevance of the 1-D assumption is therefore not only of academic interest, and there is scope in changing this commonly used model to include 3-D effects in the calculation.

Finally, most of the 1-D approaches were based on approximate expressions for the Joule heating term in the superconducting strand, simplified functional dependence of the magnetic field on the conductor and of the time dependence of the operating current. Because we were starting the development of a new model, we decided to maintain it as general as possible, so that we would be able to cope with the large number of different situations arising in the design of a fusion magnet.

0011-2275/92/070659-09

The model presented here is based on a general cable configuration formed by the parallel channels of the helium flow and several longitudinal heat and current conductors, allowing for thermal gradients in the cable cross-section. It includes the 3-D effects by permitting the heat transfer between adjacent cables. This extension has been achieved in a simple manner preserving the transparency of the basic 1-D model. Current, magnetic field and source terms (e.g. Joule heating) are arbitrary. Finite elements are used in preference to finite differences as a way to increase accuracy and flexibility.

Basic equations

For a force-flow cooled conductor the helium flow can be regarded as 1-D along the cooling channels with a good degree of approximation. We assume throughout this work that the flow always remains in single phase, a condition satisfied when supercritical helium is used as coolant. The analysis of the quench propagation requires the solution of the following equations.

Fluid flow and energy transport equations for a 1-D channel

$$\frac{\partial \rho}{\partial t} + \frac{\partial(\rho v)}{\partial x} = 0 \tag{1}$$

$$\frac{\partial(\rho v)}{\partial t} + \frac{\partial(\rho v^2)}{\partial x} + \frac{\partial p}{\partial x} = 2f\frac{\rho v|v|}{D_h} \tag{2}$$

$$\frac{\partial(\rho e)}{\partial t} + \frac{\partial(\rho e v)}{\partial x} + \frac{\partial(p v)}{\partial x} = h\frac{S}{A_{he}}(T_s - T_{he}) \tag{3}$$

$$e = i + \frac{v^2}{2} \tag{4}$$

The set of unknowns is the density ρ, the velocity v, the helium pressure p and temperature T_{he}, the total and internal energy e and i respectively. In the above A_{he} is the cross-sectional area of the helium conduit, D_h is its hydraulic diameter and S is the perimeter of the surface on which the convective heat transfer from the solid takes place at temperature T_s. The two coefficients f and h are the friction factor and the heat transfer coefficients, descriptive of the turbulent flow conditions. A state equation is needed to relate pressure and temperature to internal energy i and density ρ.

Heat conduction in the solid composite

In the general case, the following form of the conduction equation in three dimensions holds:

$$\rho C\frac{\partial T_s}{\partial t} - \nabla(K\nabla T_s) = \dot{Q}_{ext} + \dot{Q}_J \tag{5}$$

with the following convective boundary condition for the heat flux on the surface S at the interface with the helium:

$$-K\frac{\partial T_s}{\partial n}\bigg|_S = h(T_s - T_{he}) \tag{6}$$

Here the unknown is the temperature of the solid, T_s. The properties of the solid materials to be specified are the heat capacity C and thermal conductivity K. The source terms are the external heating power density $\dot{Q}_{ext}$ and the Joule heating power density $\dot{Q}_J$. Finally, n represents the direction normal to the boundary, pointing outwards.

For the present purpose it is convenient to deal only with the 1-D form of the Equation (5) combined with the boundary condition (6), written along the longitudinal conductor axis x, valid for the hypothesis of an homogeneous conductor component i with cross-section A_i, heat capacity C_i, thermal conductivity K_i and temperature T_i.

$$A_i\rho C_i\frac{\partial T_i}{\partial t} - A_i\frac{\partial}{\partial x}\left(K_i\frac{\partial T_i}{\partial x}\right) = h_l S_{i-he}(T_{he} - T_i) + \sum_j h_{ij}S_{ij}(T_j - T_i) + A_i\dot{Q}_i \tag{7}$$

The source terms on the r.h.s. of Equation (7) are respectively the heat exchange with the helium at temperature T_{he} through a heat exchange coefficient h_l and a contact surface S_{i-he}, heat exchange with another conductor j at temperature T_j through a heat exchange coefficient h_{ij} and a contact surface S_{ij}, and the density of heating power $\dot{Q}_i$ (external or Joule) per unit length.

Joule heat generation

Special attention in the superconducting composite is given to the Joule heat generation term. With reference to an electric conductor with negligible dimensions in transverse direction to the current flow, the Joule heating power is a function

$$\dot{Q}_J = \dot{Q}_J(T, B, J) \tag{8}$$

of the temperature T and the field B, in turn functions of position and time, and of the operating current density J in the conductor, dependent only on time through the solution of the circuit equations presented later*

The Joule heating $\dot{Q}_J$ is related to the current carrying capability of the conductor specified by the critical surface $J_c(B, T)$, of which two typical examples are reported in *Figure 1*. To remain as general as possible, we use the following method to compute the Joule heating term:

—for temperatures smaller than the current sharing temperature T_{cs} no resistive loss will appear and

$$\dot{Q}_J = 0 \tag{9}$$

*The Joule heat generation in the composite conductor, in reality, will also depend on the current sharing transient. During the very early stage of the *current sharing* the current flowing in the superconductor exceeding the value of J_c will have to be transferred by inductive coupling and diffusion into the copper. This phenomenon, completely described by the Maxwell equations, is of extreme complexity. However, the characteristic time constant τ_c for the conductors considered here is of the order of hundreds of μs to some ms, while the quench characteristic times are between some tens of ms (initiation) to some tens of s (development). Therefore the current transfer can be assumed as a small perturbation and neglected. This is equivalent to the assumption of an instantaneous transfer ($\tau_c = 0$).

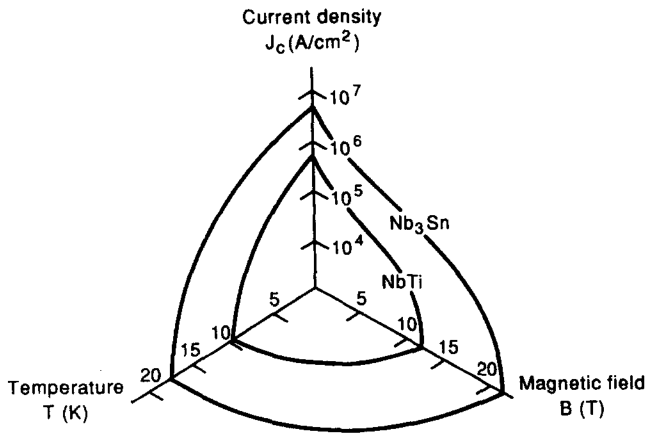

Figure 1 $J_c(B, T)$ surfaces for Nb_3Sn and NbTi

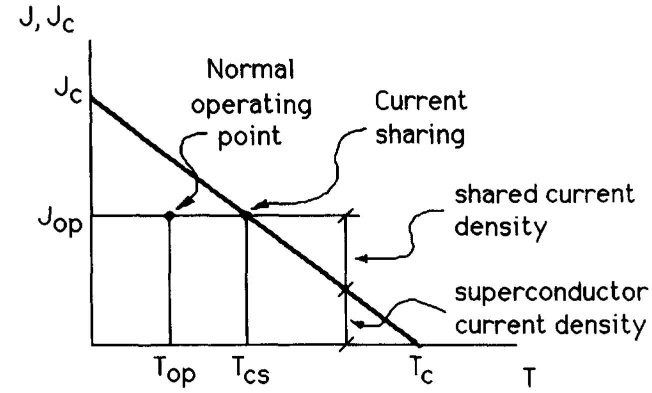

Figure 2 Operating point and definition of the current sharing temperature in the case of linear J_c *versus* T dependence. The effect of the increase of the operating temperature is also indicated by the shared current density

—for temperatures greater than the critical temperature T_c the whole loss will be concentrated in the copper

$$\dot{Q}_J = J^2 \rho_{Cu} \tag{10}$$

where ρ_{Cu} is the copper resistivity

—in the current sharing regime part of the loss will be in the copper and part in the superconductor. In this regime we can write that the total loss is

$$\dot{Q}_J = \frac{A_{Cu}\dot{Q}_{J_{Cu}} + A_{sc}\dot{Q}_{J_{sc}}}{A_{Cu} + A_{sc}} \tag{11}$$

where the Joule heating in the copper is given by

$$\dot{Q}_{J_{Cu}} = J^2_{Cu}\rho_{Cu} \tag{12}$$

and the Joule heating in the superconductor

$$\dot{Q}_{J_{sc}} = J_{Cu}\rho_{Cu}J_c \tag{13}$$

where we used J_{Cu} to indicate the current density shared by the superconductor in the copper, i.e. if I is the operating current:

$$J_{Cu} = \frac{I - J_c A_{sc}}{A_{Cu}} \tag{14}$$

The term $J_{Cu}\rho_{Cu}$ is the electric field appearing along the cable due to the resistive current sharing in the stabilizer.

Note that using the assumption of linear dependence of J_c on T one obtains for $\dot{Q}_J$ the usual expression

$$\dot{Q}_J = g\left(\frac{I_{op}}{A_{Cu}}\right)^2 \rho_{Cu} \tag{15}$$

where

$$g = \begin{cases} 0 & \text{if } T < T_{cs}; \\ \dfrac{T - T_{cs}}{T_c - T_{cs}} & \text{if } T_{cs} \le T \le T_c; \\ 1 & \text{if } T > T_c \end{cases} \tag{16}$$

where the definition of T_{cs} is given in *Figure 2*. However, Equations (11)–(13) are valid for any dependence of J_c on T and B, while Equations (15) and (16) hold only in the case of linear J_c *versus* T dependence and should be, in principle, avoided if the J_c function is completely given. Finally, the copper resistivity ρ_{Cu} must le treated consistently in the calculation as a function of magnetic field and temperature.

Circuit equations. As shown above, the heat production term depends on the current flowing in the conductor, and this must be determined at any time by the solution of the electrical network formed by the pancakes in the inductively coupled coils and the external electrical components. In the case of a set of n inductively coupled coils, with independent power supply and dump resistors, the current I_i in the ith coil will be a function of time and of the currents in the other coupled circuits I_j through the differential equation

$$\sum_j M_{ij}\frac{dI_j}{dt} + L_i\frac{dI_i}{dt} + R_iI_i = V_i \tag{17}$$

where M_{ij} and L_i are the mutual and self inductances and R_i is the total resistance of the circuit. The first two are determined by the geometry of the circuit and will remain constant throughout the evolution of the quench. The term V_i is the voltage of the external power supply. Its value depends on the preprogrammed behaviour of the power supply and on the (V, I) characteristics.

The total resistance of each circuit is a function of time as it contains the contribution of the coil internal resistance R_{quench} which develops in time as the quench front propagates and the temperature changes. Further, due to the effect of magnetic field on copper resistivity, a change in the operating current in the magnet system will also affect the coil resistance.

Magnetic field in the coil

The magnetic field in the coil, B, can be computed using the Biot–Savart law. Usually the problem is linear function of the operating current of the magnets (no ferromagnetic materials), and the field can be computed using influence matrices calculated at the beginning of the transient and stored. This increase greatly the efficiency of the calculation.

All the above equations need a consistent set of boundary and initial conditions. In particular, for the helium flow we assumed that the 1-D channels are connected to pressure reservoirs at inlet and outlet. The reservoirs represent manifolds with a large volume, but they can be assigned a pressure and temperature variation in time to model finite volume conditions. An alternative is a *symmetry* boundary condition on the flow, which also corresponds to a closed valve at the channel inlet or outlet. For the heat conduction equation, adiabatic boundaries are assumed around the coil, which is usually a sensible approximation of a well-shielded design. The calculation of the current requires the specification of the initial value of the current in the branches of the electric network, while for the magnetic field no boundary conditions are required (they are already satisfied by the Biot–Savart law).

Model

Without loss of generality, we consider the conductor configuration of *Figure 3*, representing a typical cable-in-conduit conductor[8], and the winding scheme in *Figure 4*. We can observe that the winding pack of a force-flow cooled superconducting coil presents a large anisotropy, in which we can clearly identify two main directions: the longitudinal axis of the conductor, characterized by a typical length of the order of hundreds of metres, and the transverse direction, normal to the longitudinal axis, which lies in the plane of the winding pack cross-section and with a typical length of the order of some centimetres. The modes of energy transport and propagation of a normal zone are substantially different in these two directions: in the longitudinal direction the helium flow is usually far more effective than heat conduction in propagating in the normal zone, while in the transverse direction heat conduction through cable jacket and insulation is the only mechanism responsible for the propagation. Finally, the thermal properties in the two directions are also largely non-isotropic as the longitudinal heat conductivity of a cable is greater by several orders of magnitude than the transverse one.

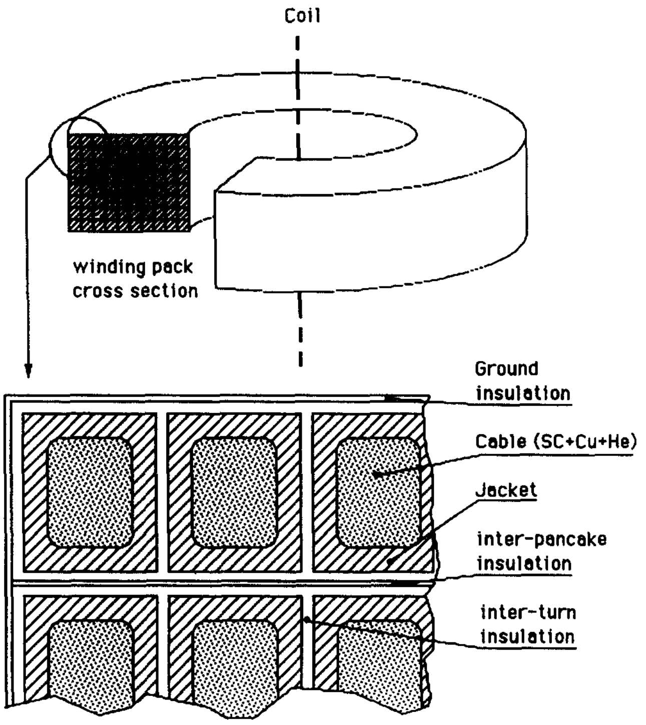

Figure 4 Schematic view of the winding pack configuration assumed

It is natural to use these properties in the formulation of the computational model. In fact, the mere application of a brute force method, involving full meshing the 3-D domain, would be highly inefficient in terms of computational costs and could give serious numerical difficulties. The approach proposed here is to discretize the coil using a set of 1-D channels, and to couple these using an appropriate model of the transverse thermal resistance of the winding pack. A schematic view of this model is given in *Figure 5*.

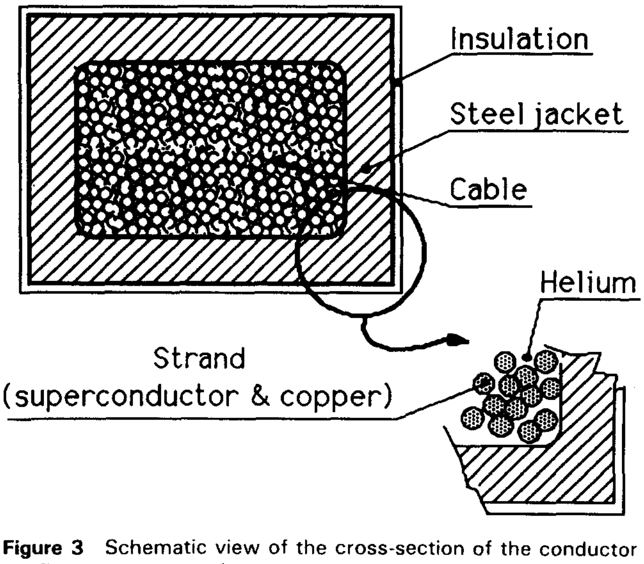

Figure 3 Schematic view of the cross-section of the conductor configuration assumed

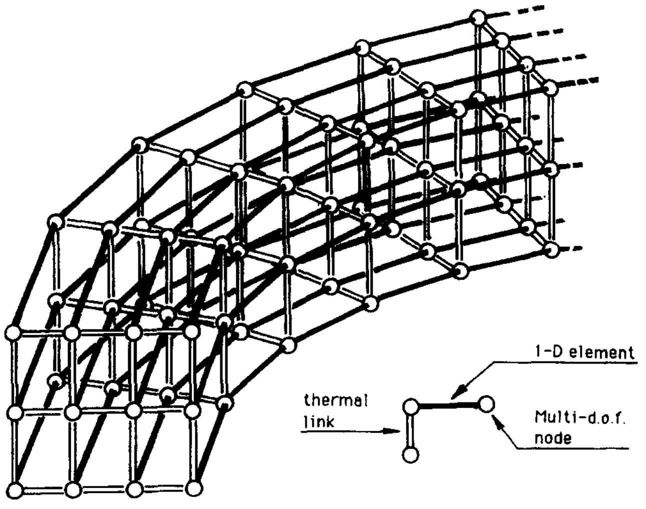

Figure 5 Approximation of the original 3-D problem with a set of coupled 1-D channels thermally linked in the cross-sections of the winding pack

Model for the 1-D channel

This is the basis of the quench analysis model, and consists of a 1-D representation of the cable in its longitudinal direction. Here the components forming the 1-D channel cross-section in which the helium flows are the superconducting strands and the assembly of jacket and insulation. The copper in the superconducting strand has a conductivity several orders of magnitude greater than that of the other components in the whole temperature range (from cryogenic temperature to room temperature). On the other hand the dominating heat capacities are those of the helium in the low temperature range (4 to 30 K) and those of steel and insulating materials (epoxy resins) in the high temperature range (30 K to room temperature).

Because of these differences in the material properties, it is not possible to combine all heat capacities and thermal conductivities. For instance, as the heat capacities change with temperature by several orders of magnitude in the range from 4 K to 50 K, the neglect of a small temperature gradient between the components of the strands in the cable (copper and superconductor) and the cable wall (jacket and insulation) could result in a large over-estimate of the total heat capacity of the cable. This is particularly true for cable-in-conduit conductors, where the steel and the surrounding insulation are not in direct, intimate thermal contact with the strands, but exchange heat mostly through the helium. In our model we assumed that the copper and superconductor in the strand have the same temperature by virtue of the large thermal conductivity of copper. At the same time the helium temperature in the channel will also be uniform, as in general the flow is highly turbulent and therefore involves a large degree of mixing. With regard to the jacket and insulation we approximated the temperature distribution by a uniform average temperature. The effects of the temperature gradients in the cable cross-section are taken into account, at least up to the first order, by separating the three components: strands, helium and jacket. The strands and the jacket are both in thermal contact with the helium, which acts as the main thermal coupling between them. In addition it is assumed that strands and jacket are in direct contact on a portion of their surface, thus adding a further thermal coupling term. The resulting model is simple to treat, and physically more realistic than that obtained by combining the heat capacities in one single point.

The model for the 1-D analysis is shown in *Figure 6*. The heat conduction equation (7) has to be converted into the following two equations for the strands and jacket respectively:

$$A_{st}\rho C_{st}\frac{\partial T_{st}}{\partial t} - A_{st}\frac{\partial}{\partial x}\left(K_{st}\frac{\partial T_{st}}{\partial x}\right) = h_1 S_{st-he}(T_{he} - T_{st}) + h_2 S_{st-jk}(T_{jk} - T_{st}) + A_{st}(\dot{Q}_{ext} + \dot{Q}_J) \quad (18)$$

$$A_{jk}\rho C_{jk}\frac{\partial T_{jk}}{\partial t} - A_{jk}\frac{\partial}{\partial x}\left(K_{jk}\frac{\partial T_{jk}}{\partial x}\right) = h_1 S_{jk-he}(T_{he} - T_{jk}) + h_2 S_{st-jk}(T_{st} - T_{jk}) \quad (19)$$

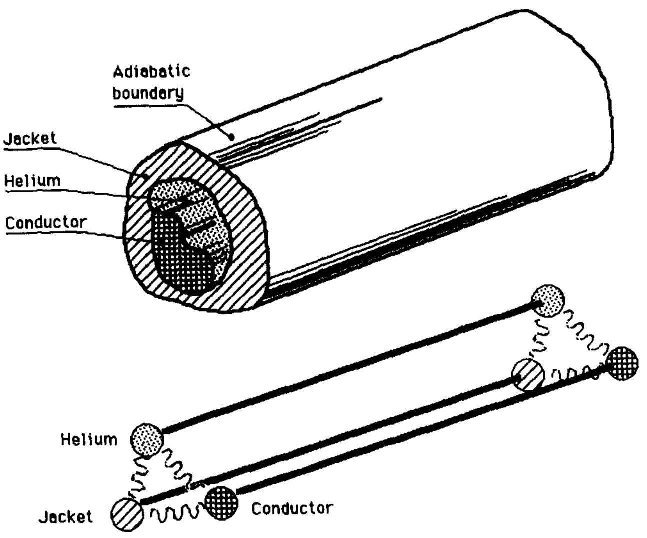

Figure 6 Schematic view of the 1-D model used for the conductor in the longitudinal direction

Equation (18) refers to the strand (subscript st), while Equation (19) is for the jacket and insulation (subscript jk). Note that for the contact to the helium and for the inner contacts of strands and jacket two different heat transfer coefficients have been used in the two equations above. In fact the heat transfer to the helium is substantially different from that at the contact surface between strands and jacket. The first, h_1, is defined using turbulent correlations, while the second, h_2, can be obtained only from measurements of thermal resistance and depends on the type of contact. Note also that in Equation (19) no source term has been included. In fact the external heating sources are usually located in the strands and the Joule heating in the jacket is negligible due to its high electrical resistivity at cryogenic temperatures.

The thermal properties for Equations (18) and (19) are obtained as weighted averages; in particular the density is given by the area weighted average of the densities of the single components

$$\rho = \frac{\Sigma_{i=1}^{n}\rho_i A_i}{\Sigma_{i=1}^{n} A_i}$$

The thermal conductivity is treated similarly

$$K = \frac{\Sigma_{i=1}^{n} K_i A_i}{\Sigma_{i=1}^{n} A_i}$$

while the heat capacity is given by the mass averages

$$C = \frac{\Sigma_{i=1}^{n}\rho_i C_i A_i}{\Sigma_{i=1}^{n}\rho_i A_i}$$

3-D model of the coil

The geometry of the jacket and the insulation between two adjacent cable spaces resembles very closely the situation of a composite slab. Therefore an approximation to the heat transfer in the winding pack can be

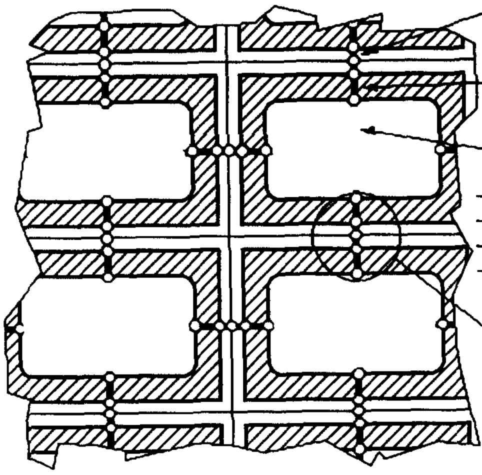

Figure 7 Equivalent multi-link model for the heat flux in the winding pack. The sandwich of jacket and insulation is substituted by a series of thermal resistances with degrees of freedom lumped at the centre of each layer of the sandwich

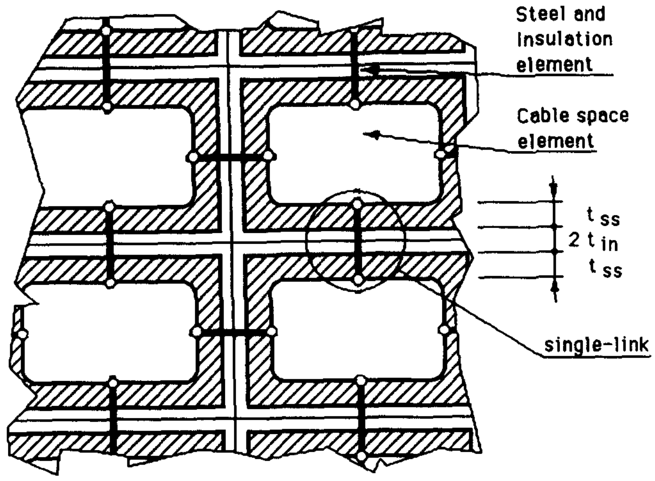

Figure 8 Equivalent single link model for the heat flux in the winding pack. This is the lowest level of approximation that can describe the heat flow between cables

obtained substituting each portion of jacket and insulation between two conductors with an equivalent slab having the same average length in the direction normal to the heat flux. With this simplification the heat diffusion in the winding cross-section can be regarded as a set of independent 1-D problems between the cable spaces.

The 3-D quench propagation can therefore be reduced to a set of 1-D problems with nodal links obtained through the heat conduction in 1-D through the composite slabs, as shown in *Figure 7*. The thermal links are located between nodes of adjacent turns in each pancake, and between nodes belonging to the same turn but in adjacent pancakes. Only conductors with adjacent faces are coupled, meaning that the heat flux across the corners of the cables is neglected.

The heat transfer in each composite slab presents a relatively easy problem, which could be solved again by discretization of the domain into finite elements. Nevertheless, it is advantageous to go further with the simplification, reducing the number of elements needed for the solution. Each multiple layer slab could be assimilated to a single layer link, with an equivalent heat conductivity, or thermal resistance, and heat capacity. The thermal resistance and the heat capacity should be chosen in such a way to guarantee the dynamic equivalence between multiple and single links, that is to say that both the steady state and transient effects on the temperature distribution should be considered in the lumping. The last level of approximation is therefore constituted by a set of 1-D channels cross-coupled, turn to turn and pancake to pancake, through a single layer link with given (non-linear) thermal resistance and heat capacity as shown in *Figure 8*. The amount of saving is clear, but two questions still have to be answered:

- How good is the approximation of 1-D heat flux in the jacket and insulation of each cable?
- How shall we choose the values of thermal properties of each link in order to get the response which resembles in a close manner that of the original system?

The answer to these two questions has to be sought in the fields of the substructuring[9] or model reduction techniques[10], as the procedure proposed consists of the reduction of the number of degrees of freedom of the problem.

Instead of using the rigorous formulation of the problem let us come back again to the simple analogy with the 1-D slab. In steady state conditions, assuming that the properties are linear it is possible to define the heat resistance of the 1-D slab as

$$h = \frac{1}{\Sigma_i \frac{L_i}{K_i}} \tag{20}$$

and the heat flux through the slab is equal to

$$\dot{q}'' = h\Delta T \tag{21}$$

where ΔT is the temperature difference across the slab. For a steady state non-linear problem it is possible to use a reasonable approximation of the thermal resistance by performing a further subdivision of the slab in portions with nearly constant thermal conductivity. The limit of this procedure is the differential equivalent of Equation (20).

$$h = \frac{1}{\int_x \frac{dx}{K(x)}} \tag{22}$$

Although these simple results are only valid in steady state conditions, we can assume that they give a good approximation of the dynamic behaviour in the time scale of interest. In fact, during a transient, the temperature distribution and the heat flux will tend asymptotically to the steady state solution. In this aspect, the steady state can be regarded as the mode with the lowest frequency (apart from the thermal equivalent of

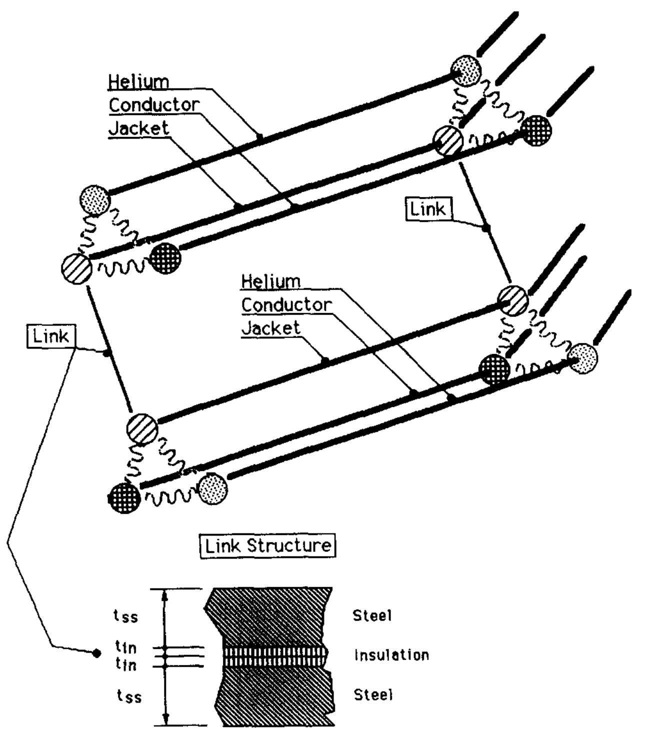

Figure 9 Schematic view of the details of the coupled 1-D channels equivalent to the initial 3-D problem. The internal structure of the coupling links is shown

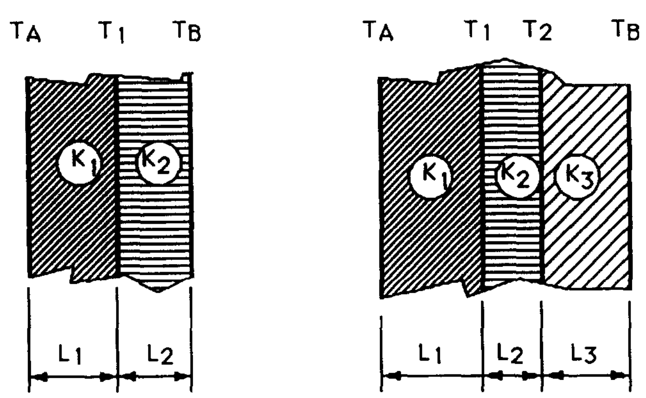

Figure 10 Configurations considered for the calculations of the thermal resistance of the links. The values of the temperature at the boundaries of the slab are given

a rigid body displacement). Tests performed in relevant geometries and under relevant initial boundary conditions have shown that the situation can be closely modelled by a 1-D slab in steady state[11,12].

A detailed view of the resulting model for the coil is given in *Figure 9*, where the structure already shown in *Figure 5* is expanded.

For the calculation of the value of the thermal resistance of the link, two types of composite structure have been considered: a two-layer slab and a three-layer slab. The first is the case of two cables in direct contact at their jackets, the second that of the jacket–insulation–jacket sandwich. Given the temperature at the boundaries of the slab, T_A and T_B in *Figure 10*, the steady state value of the temperature in the interior points is easily calculated in the approximation of linear properties. In the case of the two-layer composite, we have

$$T_1 = \frac{\frac{K_1}{L_1} T_A + \frac{K_2}{L_2} T_B}{\frac{K_1}{L_1} + \frac{K_2}{L_2}} \tag{23}$$

while for the three-layer composite

$$T_1 = \frac{\frac{K_1 K_2}{L_1 L_2} T_A + \frac{K_1 K_3}{L_1 L_3} T_A + \frac{K_2 K_3}{L_2 L_3} T_B}{\frac{K_1 K_2}{L_1 L_2} + \frac{K_1 K_3}{L_1 L_3} + \frac{K_2 K_3}{L_2 L_3}} \tag{24}$$

$$T_2 = \frac{\frac{K_1 K_2}{L_1 L_2} T_A + \frac{K_1 K_3}{L_1 L_3} T_B + \frac{K_2 K_3}{L_2 L_3} T_B}{\frac{K_1 K_2}{L_1 L_2} + \frac{K_1 K_3}{L_1 L_3} + \frac{K_2 K_3}{L_2 L_3}} \tag{25}$$

Once the temperature at the interior is known, it is possible to compute the value of the average thermal conductivity of each layer. To simplify matters, the value of K is computed at the average temperature of the layer. In fact the solution of Equation (23) or of Equations (24) and (25) requires an iterative procedure. Direct iteration can be performed quite efficiently (generally three to four iterations are enough to reach a relative error of less than 10^{-3} of the heat flux). Once the solution has converged the thermal resistance is computed using Equation (20). This is finally used to compute the equivalent heat transfer between adjacent conductor jackets, according to Equation (21).

Initial conditions

The initial condition for a coil in which a quench starts is, in general, that of normal operation. The coil is cooled by a steady flow of helium under given heat loads. In the model considered here the distribution of the variables should be computed along the channel. As we have chosen an explicit solution method for the helium flow a relaxation procedure could be used letting an initial, arbitrary distribution (e.g. zero flow) evolve to the natural steady state. This is feasible but time consuming, as the time stepping should cover at least a couple of residence times of the coolant in the cooling path to achieve a steady state condition. Therefore an approximation is used for the determination of the initial steady state distribution in the channel. Neglecting all the time derivatives in Equations (1)–(3) and assuming that the heat diffusion in the conductor (Equations (18) and (19)) is negligible, the resulting set of equations is much easier to solve: the mass flow is constant (from the steady state continuity equation), and for relatively small flows (as in typical technical applications) the pressure drop is given by

$$\frac{\partial p}{\partial x} \approx 2f \frac{\rho v^2}{D_h} \tag{26}$$

where the compressibility effects have been neglected. The energy equation can be written in terms of enthalpy of the fluid $h = i - (p/\rho)$

$$\dot{m}\frac{\partial h}{\partial x} \approx A_s \dot{Q}_{ext} \quad (27)$$

where again the compressibility terms have been neglected. An approximate solution of the two equations above can be achieved assuming that the r.h.s. of Equation (26) is constant along the pipe length. In this case the pressure distribution is linear along the length and the pressure drop is given by

$$\Delta p = 2f\frac{\rho v^2}{D_h}L \quad (28)$$

where L is the pipe length. The enthalpy distribution is also easily computed from Equation (27) by integration of the external heating, which is an assigned function of space. The local values of pressure and enthalpy uniquely determine all the other variables of the helium. Helium temperature and density are therefore known, and the latter can be used to determine the flow velocity in the assumption of constant mass flow. The conductor temperature is then set equal to that of helium, assuming that in steady state the temperature gradients between conductor and helium must be small.

Method of solution

For the solution of the helium flow and of the heat conduction along the conductor longitudinal axis we used the finite element method[13] (FEM). This has the advantage of giving higher accuracy and more modelling freedom than, for instance, the finite difference approximations of the governing equations. The 1-D model of the cable cross-section was translated into a finite element with three thermal degrees of freedom per node: strand, helium and jacket temperature. In addition to these, the flow variables were defined at the helium nodes. The 1-D channels were obtained by assembly of these elements. Note that the element can be easily modified to take into account other conductor configurations, e.g. the case of several independent cooling channels in the conductor, or to model better the jacket structure, subdividing it into layers of steel and insulation[6].

The solution of the helium flow was based on an explicit two-step form of the Taylor–Galerkin algorithm[12–14], which offered optimal compromises among accuracy of the integration, CPU cost and programming simplicity. For the heat conduction equation an implicit solver was used. Implicit treatment was implemented also in the heat exchange among the components of the 1-D element, while explicit coupling was used among the channels, to form the 3-D assembly. This choice was justified by the fact that the time constants of the heat transfer with the helium are very small (of the order of one millisecond) compared to those of the heat transfer among conductors in the winding pack (typically some tenths of a second). Therefore, the simplification of the data structure was obtained without major penalties due to the conditional stability of the explicit parts of the solution algorithm. In fact, the strictest requirements on the time step were dictated by the algorithm used in the solution of the helium flow.

The circuit equations were solved by standard techniques adopted in initial values and ordinary differential equations, and the coupling to the thermal-hydraulic analysis was achieved explicitly. This also posed no serious problem for stability and consistency of the algorithm, as the time constants of the electrical circuits modelled are in general several orders of magnitude larger than those involved in the quench propagation. Finally, the magnetic field was computed at each time step by means of preprocessed influence matrices, whose coefficients link the field at any point to the current in the circuital branch.

The final algorithm could be broken in modules performed independently at each time step, so that there is a great potential for parallel processing and speed increase. In fact, great attention was devoted to achieving a sufficient CPU speed to allow dealing with very large problems arising when a whole coil is modelled. Material properties and helium property routines were also subject to this optimization process to guarantee that even with extremely large problems (e.g. a complete coil) a solution could be obtained in reasonable computing time (some CPU hours).

Conclusion

The model presented for the analysis of quench in superconducting, force-flow cooled magnets advances substantially those previously used as it allows inspection of the thermal gradients in the cable and includes transverse heat transfer among conductors in the winding pack. The solution of the coupled heat diffusion and helium flow has been successfully reduced to sets of simplified coupled 1-D problems equivalent to the original configuration. The formulation of the 1-D problem given here is appropriate for the analysis of a coil wound from cable-in-conduit conductors. A treatment similar to that proposed here could be used to extend the 1-D model to other situations, e.g. other conductor configurations, provided that the 1-D analogue is a good description of the original 3-D problem.

The method proposed has been implemented into a code which is able to solve the full problem of the quench propagation in a 3-D configuration, also taking into account the operating current and magnetic field changes by means of integrated circuital and magnetostatic solvers. We believe that at the moment this is the most versatile and comprehensive simulation model for force-flow cooled superconducting magnets. An extensive numerical and experimental validation program is under way to check that the assumptions and the solution algorithms have a sound physical basis. Part II of this paper gives examples of applications in relevant conditions.

References

1 **Wilson, M.N.** *Superconducting Magnets*, Clarendon Press, Oxford (1983)

2 The Next European Torus (NET) *Fusion Technol* (1988) **14** 1

3 **Arp, V.** Computer analysis of quench transients in force-flow cooled superconductors for large MHD magnets *Proc Superconducting MHD Magnet Design Conference*, MIT, Cambridge (1978)

4 **Marinucci, C.** A numerical model for the analysis of stability and quench characteristics of force-cooled superconductors *Cryogenics* (1983) **23** 579–586

5 **Cornelissen, M.C.M. and Hoogendoorn, C.J.** Propagation velocity for a force cooled superconductor *Cryogenics* (1985) **25** 185–193

6 **Wong, R.L.** Program CICC flow and heat transfer in cable-in-conduit conductors, presented at 13th Symp. on Fus. Eng., Knoxville, TN (October 2–6, 1989)

7 **Luongo, C.A., Loyid, R.J., Chen F.K. and Peck, S.D.** Thermal-hydraulic simulation of helium expulsion from a cable-in-conduit conductor, *IEEE Trans Magn* (1989) **25** 1589–1595

8 **Hoenig, M., Iwasa, Y. and Montgomery, D.B.** Supercritical-helium cooled 'bundle conductors' and their applications to large superconducting magnets *Proc 5th Int Conf on Magnet Technology*, Frascati (1975)

9 **Guyan, R.J.** Reduction of stiffness and mass matrices *AIAA J* (1965) **3** 380

10 **Ben Jaafar, M.T., Pasquetti, R. and Petit, D.** Model reduction for thermal diffusion: application of the Eitelberg, Marshall and aggregation methods to a heat transfer transmission tube model. *Int J Numer Meth Eng* (1990) **29** 599–617

11 **Bottura, L.** 2-D simulation of quench propagation for force-flow conductors *IEEE Trans Magn* (1991) **27** 1904–1907

12 **Bottura, L.** The numerical solution of quench in superconducting magnets, *PhD Thesis* submitted to the University of Wales, University College of Swansea, Wales, UK (1991)

13 **Zienkiewicz, O.C. and Taylor, R.L.** *The Finite Element Method*, Vols 1 and 2, 4th Edn McGraw Hill, New York (1989–1991)

14 **Peraire, J., Peiro, J., Formaggia, L., Morgan, K. and Zienkiewicz, O.C.** Finite element Euler computations in three dimensions, *Int J Numer Meth Eng* (1988) **26** 2135–2159